Polyelectrolyte MCs for light triggered therapy and imaging

Catarina Lourenço Costa

Under supervision of: Doctor Suzana Maria de Andrade Sousa Paiva

Instituto Superior Técnico, Universidade de Lisboa, Lisboa, Portugal September 2020

Aiming the development of a mechanism for the transport of porphyrins, increasing the efficiency of photodynamic therapy (PDT) and its potential application in bioimaging, MCs were developed with specific coating consisting polyelectrolyte, PSS and PAH layers, *meso*-tetrakis (*p*-sulfonatophenyl) porphyrin (TSPP), and rhodamine 6G. The incorporation of rhodamine has the objective of promoting the increase in fluorescence of the porphyrin, by itself a weak emitter, by non-radioactive energy transfer (a process known as FRET, Förster Resonance Energy Transfer). The effect of the porphyrin / R6G relative position on the stability of the layer-by-layer generated systems was studied, and by FLIM, energy transfer was verified between the two species integrated in the polyelectrolyte matrix adsorbed in the MCs. The adsorption of oppositely charged PEs was followed by measurement of the zeta potential. The functionalization and characterization of the optical and electronic properties of the hybrid system was followed by steady-state fluorescence and resolved over time and compared with systems containing only porphyrin or rhodamine, and with the same species in solution. The acquisition of images by fluorescence confocal life time microscopy (FLIM) allowed to observe energy transfer, responsible for exciting porphyrin, which in turn, in oxygenated environments can proceed by a photochemical pathway involving energy transfer between the excited state photosensitizer triplet and triplet oxygen, producing a very reactive specie with efficient cytotoxic action, singlet oxygen.

1. INTRODUCTION

In 2018, Portuguese population registered around 58 199 cancer cases, from which 28 960 resulted in human loss, the highest mortality cancers are colorectum (14.7%) and lung cancer (16.1%). Globally, according to World Health Organization (WHO), cancer represents the second leading cause of death, accounting for an estimated 9.6 million deaths, or one in six deaths, in 2018 [1]. Depending on the type and stage of cancer, the selection of appropriate treatment often requires the use of multi-treatment modalities, like surgery and chemotherapy. Surgery can imply infections damaging the nearby tissues and is not effective for metastasis. Chemotherapy is a standard cancer therapy, however, due to poor targeting and lack of selectivity of this treatment, it damages healthy cells, the patients develop resistance to chemical agents, and have considerable toxic and severe side effects. Thus, it has become an urgent need to develop new economically viable cancer therapies and detection methods, to be applied with spatial-, temporal- and dosage-controlled ways on the early stages of this disease.[2] Photodynamic Therapy (PDT) addresses some drawbacks of the nowadays available treatments, with lack of long-term toxic effects, and minimal invasiveness, this therapy has given a positive glance towards the research activity

in the field, aiming its improvement. Porphyrins are a unique and diverse class of compounds widely available in nature, offering a variety of opportunities spanning various diagnostic and therapeutic modalities, applied in PDT as photosensitizers.[3] By taking advantage of their known tuneable specific composition and reproducible synthesis, photophysical properties, biocompatibility, and biodegradation, with shown preferential retention on tumour tissues they provide functionalities as cargo tracking and activatable phototoxicity. Polyelectrolyte (PE) multilayer capsules designed Layer-by-Layer, with active elements for targeting, labelling, sensing, and delivery represent a great promise for controlled delivery of drugs and the development of new sensing platforms. These biodevices should be biocompatible materials, like CaCO3 colloid templates, that once exposed to a specific stimulus (e.g., pH variation, or light irradiation), undergo a gradual release of the shell components. Preferential accumulation mechanisms of porphyrins in tumor cells are explained based on low-density lipoprotein receptors theory and pH difference. Lipophilic porphyrins bind to the centre of low-density lipoprotein receptor, entering tumour cells through a specific membrane receptor, apolipoprotein B. The aim of the present Thesis is to design a double functionalized polyelectrolyte coated colloidal system with a porphyrinic photosensitizer, *meso*-tetrakis (*p*-sulfonatophenyl) porphyrin (TSPP), and rhodamine 6G .This MCs systems are expected to maintain the monomeric form of the photosensitizer (porphyrin), to prevent self-quenching, and further improve the selective aggregation of porphyrin in target sites to enhance the local anticancer effect. R6G expected role is to, upon excitation, transfer excitation energy by FRET to the acceptor molecules of TSPP. The success of this energy transference mechanism is related to the dipole orientation of both donor and acceptor molecules. Both PEs, PSS and PAH might orientate the dipoles of the dyes' molecules in a favourable way, such that the FRET, Förster Resonance Energy Transfer, process is efficient. When in vivo, the porphyrin, as the acceptor of the excitation energy undergoes a Type II photochemical process involving an energy transfer between excited triplet state of the PS and stable triplet oxygen, resulting in ROS that can evoke some cell death pathways.

2. EXPERIMENTAL PROCEDURES

Materials Poly(sodium 4-styrenesulfonate) [PSS (MW~75000, 18% wt % in water)] and poly(allylamine hydrochloride) [PAH (MW~17500)], obtained from Sigma-Aldrich. Sodium chloride [NaCl (MW~58,44, ≥99,5% purity)], obtained from Fisher Chemical. Sodium carbonate [Na_2CO_3 (MW~105,99)] obtained from J. T Baker. Calcium chloride [$CaCl_2$ (MW~147,02)] obtained from Merck. Sodium Hidroxide [NaOH (MW~40,00)], chloride acid [HCl (7%)] obtained from Sigma Aldrich for pH ajusts. Meso-(tetrakis)-(p-sulfonatophenyl) porphyrin [TSPP (MW~1022,908)] was obtained from Fluka (≥98% purity), Rhodamine 6 G, [R6G (MW~443,564)]) was obtained from Radiant Dyes & Accessories, and Sodium dihydrogen phosphate monohydrate

[$NaH_2PO_4.H_2O$ (MW~137,99)] obtained from Riedel-de-Haen. Polyelectrolyte solutions PSS (3 mg/mL, 0,5M NaCl), and PAH (13 mg/mL, 0,5 M NaCl) were prepared in bi-distilled H_2O, and the pH was adjusted to 6.4 (for PSS/PAH polyelectrolyte microcapsule preparation). Porphyrin solution TSPP (1,25 mg/L) pH was adjusted to 8 with NaOH addition, and rhodamine R6G solution (125μM) was prepared with no pH adjust since the specie nature doesn't change with pH. The salt solution $NaH_2PO_4.H_2O$ 0,68% (w/v), pH=7,2 was prepared for the release studies.

Preparation of the $CaCO_3$ templates $CaCO_3$ colloidal templates were prepared by co-precipitation of $CaCl_2$ (0,33M, 1mL) and same volume solution of Na_2CO_3 (33M, 967μL) with PSS (6,6 g/L, 33 μL), under vigorous stirring for 30 seconds. The suspension was left during 15 minutes at room temperature. The $CaCO_3$ templates were recovered after supernatant removal by three washing/ centrifugation cycles with bi-distilled H_2O (3000 rpm, 2min). [5]

Polyelectrolyte layer-by-layer assembly-PE shell assembly The $CaCO_3$ microparticles were dispersed in aqueous solution of polyelectrolyte (1mL, C_{PSS}=3mg/mL, C_{PAH}=13mg/mL, 0,5M NaCl, pH 6,4). After stirring for 20 minutes, the resulting particles were recovered by three washing/ centrifugation cycles with bi-distilled H_2O (3000 rpm, 2 min), to remove residual polyelectrolyte. Between the centrifugation cycles vortex and ultrasounds were applied, so that $CaCO_3$ particles would be suspended in the bi-distilled washing H_2O. The assembly's order of each polyelectrolyte layer varied according to the system architecture. The alternate adsorption of the oppositely charged PEs started always with the negative PE PSS. To guaranty the potential stability of the colloidal system, measured by the zeta-potential the first layer of PAH consists of three additions of PAH; furthermore, three washing/ centrifugation cycles with bi-distilled H_2O was performed for 15 minutes, 6000 rpm. [5]

Porphyrin adsorption onto PE MCs TSPP was adsorbed onto the PE shell with PAH as the last layer. The polyelectrolyte shell MCs were suspended in a TTSPP solution (0,25mg/L) pH 8, and the system was left stirring for 1,5 hours at room temperature. Afterwards, three cycles of washing/centrifugation (3000 rpm, 2 min) were performed with bi-distilled H_2O, to recover the porphyrin-polyelectrolyte shell cores and discard non-adsorbed porphyrin, and free polyelectrolyte molecules in the solution. [5]

Rhodamine adsorption onto PE MCs R6G was adsorbed onto the PE shell with PSS as the last layer, suspending the MCs in a solution 0.046mM R6G and 1.2mg/mL of PSS. The polyelectrolyte shell MCs were suspended in the R6G solution, the system was left stirring for 1.5 hours at room temperature. To remove free non-adsorbed rhodamine and free polyelectrolyte molecules in the solution, three washing/centrifugation cycles (3000 rpm, 2 min) were performed with bi-distilled H_2O.

Polyelectrolyte MCs porphyrin and rhodamine release MCs with both porphyrin and rhodamine adsorbed in distinct PE layers suspended in a release solution, salt solution $NaH_2PO_4.H_2O$ 0,68% (w/v) physiological pH=7,2, under stirring.

Released porphyrin and rhodamine are recovered over time by collecting the supernatant after centrifugation (3000 rpm, 4 min). The medium is renovated after each sample collection. [6]

Methods A Lambda 35 spectrophotometer from PerkinElmer was used in UV-Vis absorption measurements. Fluorescence emission was recorded with a Fluorolog FL-1040 spectrofluorimeter from Horiba Jobin Yvon. Zeta potential values were measured in a Doppler electrophoretic light scattering analyzer Zetasizer Nano ZS from Malvern Instruments Ltd. pH adjustments were performed in Denver Instrument Model 15 sensor and Mettler Toledo AG 30281915 Rev A electrode, at 21ºC. STEM images were obtained by a HR-(EF)TEM JEOL 2200FS microscope with an energy dispersive X-ray spectrometer (EDS) incorporated. FLIM measurements were performed with a time-resolved confocal microscope, MicroTime 200 from PicoQuant GmbH. The excitation energy at 639 nm and 480 nm was provided by pulsed diode laser at a repetition rate of 40 and 20 MHz, respectively. The fluorescence lifetime was detected with a single-photon counting avalanche diode (SPAD) from PerkinElmer, whose signal was processed by TimeHarp 200 TC-SPC PSboard from PicoQuant working in a time-tagged time resolved (TTTR) operation mode. The Olympus IX 71 inverted microscope coupled with a water immersion objective allowed an optical analysis. With a QE Pro from Ocean Optics photoluminescence spectra were collected.

3. RESULTS AND DISCUSSION

The TSPP and R6G behaviour with PEs, PSS and PAH in aqueous solution was studied prior to their assembly in the MCs. After the solution studies, the next procedure was the design an assembly of the MCs. In the end of this experimental work, the release study of TSPP adsorbed in MCs, at pH 7.2 media.

TSPP and R6G interaction with both PSS and PAH in solution

TSPP behaviour

TSPP interaction with PAH results in the formation of H-aggregates -blue-shifted Soret peak at 401 nm and the porphyrin emission quenching. The porphyrin/PSS interaction isn't favourable since both have anionic nature. Competition between TSPP and PSS for PAH show PEs have higher affinity for each other. [7][8]

R6G behaviour

R6G interaction with PSS leads to a red-shift of the dye's maximum absorption band to ~534 nm. High [PSS] prevent R6G from aggregation.R6G/PAH interaction isn't favourable since both have cationic nature. Competition between R6G and PAH for PSS show PEs have higher affinity for each other [9].

FLIM

Resorting to FLIM, the TSPP-R6G behaviour with PEs was also studied. The temporal variation of the emission spectra seems to show the photodegradation of the acceptor molecule, the porphyrin (TSPP), whereby there will be less molecules extinguishing the donor molecules, rhodamine (R6G). This will cause the increasing of the R6G fluorescence signal (fig. 3)

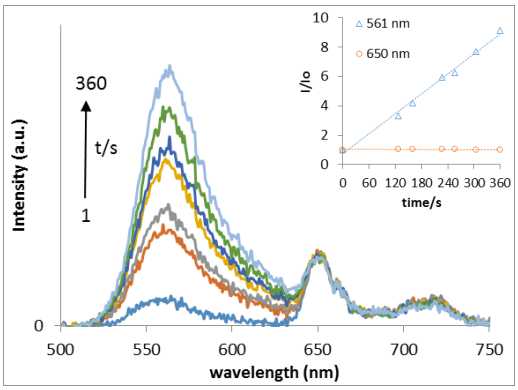

Figure 3. Fluorescence emission spectra of R6G/TSPP/PAH/PSS (1:1:2:2), obtained with λ_{exc}=483 nm at different excitation times (from 0s to 6 min). Inset shows the intensity variation with time for the λ_{em}=650 nm and λ_{em}=561 nm.

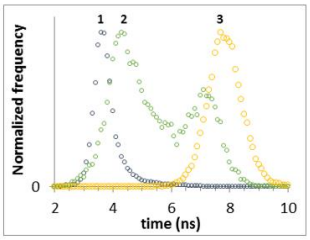

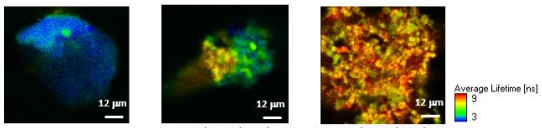

1- R6G/TSPP 1:2

2- R6G/TSPP/PSS/PAH 1:1:0,2:0,2

3- R6G/TSPP/PSS/PAH 1:1:2:2

Figure 4. Fluorescence lifetime histogram of the systems 1- R6G/TSPP 1:1 in water; 2- R6G/TSPP/PSS/PAH 1:1:0,2:0,2 and 3- R6G/TSPP/PSS/PAH 1:1:2:2 and corresponding FLIM images.

The FLIM images, figure 4, show heterogeneity for the R6G/TSPP system, since there's occurrence of blue pixels associated with average lifetimes of about 3 ns and green pixels associated with average lifetimes of about 4 ns, which might be assigned to R6G molecules aggregated, probing hydrophobic surrounding and both monomeric rhodamine, respectively. The quantum yield of porphyrin was obtained through a relative determination method explained in the experimental methods section. As can be seen for the R6G/TSPP system in solution, there is no FRET process occurring: the rhodamine signal appears with a quantum fluorescence yield $\phi_{st} = 0.95$, higher than for TSPP, $\phi_x = 0.1$ .When PEs are present in the solution, in higher concentrations (figure 4, 3), the distance between dipoles is the ideal for the efficiency of the FRET process, therefore only the acceptant molecule, TSPP, is detected (although preferably performing the excitation of the donor molecule, R6G). When PEs are present in solution, but at low concentrations (figure 4, 2), there's lower efficiency of the FRET process, and some donor is still detected. The fluorescence lifetimes obtained by FLIM corroborate this, shown that the prevalent population (36%) has a discrete lifetime of 10.3ns, which is the approximately the average lifetime of TSPP in its monomeric form at pH 7 in water. Therefore, these are promising results for the next step of coating these dyes in MCs.

Preparation of Polyelectrolyte MCs

To overcome the hydrophobic character and easy aggregation of porphyrins under physiological conditions, aiming the target accumulation selectivity for diseased tissues, colloidal carriers such as $CaCO_3$ [10][11] particles were studied and functionalized in three different designs.

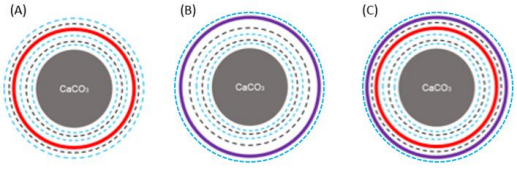

Figure 5. The structure of the three systems studied: (A)$CaCO_3$(PSS)(PAH)(PSS)(R6G)(PAH)(PSS); (B)$CaCO_3$(PSS)(PAH)(PSS)(PAH)(TSPP)(PSS); (C)$CaCO_3$(PSS)(PAH)(PSS)(R6G)(PAH)(TSPP)(PSS).

CaCO3(PSS)(PAH)(PSS)(R6G)(PAH)(TSPP)(PSS)

The loading of R6G was assured by the zeta potential [12] ʒ(CaCO3-PSS-PAH-PSS-R6G-PAH)=+29.7 mV. The zeta potential for the hybrid system was ʒ(CaCO3-PSS-PAH-PSS-R6G-PAH-TSPP)=12 mV. As the decided order for the functionalization end up putting TSPP after R6G, aiming the easing of release of the porphyrin through media, it was decided to coat with a PSS layer at the end of the system to prevent aggregation of TSPP, ʒ(CaCO3-PSS-PAH-PSS-R6G-PAH-TSPP-PSS)=-18 mV. The TEM images for this system revealed MCs with approximately the same shape and size, figure 7.

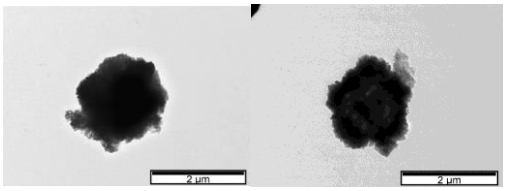

Figure 7. TEM images of CaCO3(PSS)(PAH)(PSS)(R6G)(PAH)(TSPP)(PSS).

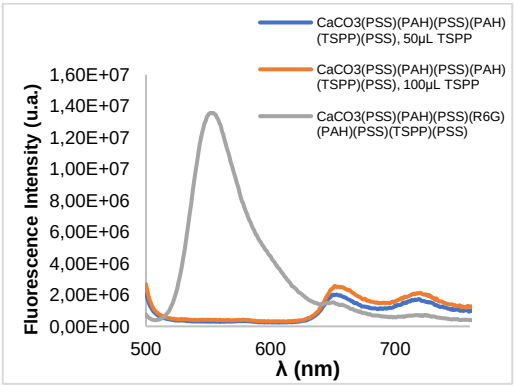

Figure 8. Emission spectra of CaCO3(PSS)(PAH)(PSS)(R6G)(PAH)(PSS)(TSPP), the hybrid system, and comparison with the porphyrin coated system λ_{exc}=483 nm, pH=7, slit 5/5 for the TSPP coated system (blue) and for hybrid system (orange).

The UV-Vis absorption spectra shown considerable light dispersion, and the impossibility to infer about absorption data. Since there's no abs data the ratio of fluorescence intensity and maximum OD, wasn't obtained. The emission spectra (figure 8) above show evidence that rhodamine was adsorbed to the capsule since its emission peak appears at ~556 nm. Two other quenched bands can be observed at ~650nm and ~720nm which correspond to the porphyrin emission bands in the CaCO3(PSS)(PAH)(PSS)(TSPP) system studied before, corroborating the porphyrin adsorption onto the MCs. Fluorescence decays of the MCs containing the hybrid rhodamine – porphyrin molecules were obtained at two distinct excitation wavelengths, 483nm exciting preferentially R6G and 638 nm suitable for preferential excitation of TSPP (table 6). In both cases, a tri-exponential fitting was the one best describing the data. A long component around 10 ns can easily be assigned to the porphyrin in an aqueous environment. This component is the one prevailing at 638nm, as expected. The intermediate component can be assigned to R6G, the value of 3.86 is analogous to that of the dye alone in MCs, however, this component appears quenched in the hybrid upon excitation at 483 nm. This quenching can tentatively be assigned to a process of dynamic quenching taking place through energy transfer profiting from a suitable distance between the two probes provided by the assembly of the PE MCs. Under these conditions, the orientation of the donor emission dipole (R6G) and that of the acceptor absorption dipole (TSPP) is such that the energy transfer process is more efficient than the R6G radiative emission, leading to a quenching in R6G fluorescence emission. Another important characteristic of this system that further contributes to the prevalence of the resonance energy transfer

is the important overlapping of the emission spectrum of the rhodamine and the absorption spectrum of TSPP [4].

FRET

Förster Resonance Energy Transfer is based on an excited state donor D transfering energy to a ground state acceptor A through long-range dipole–dipole interactions. D and A must be 10–100 Å close, and their transition dipole orientations cannot be perpendicular. In addition, there must be an overlap of donor emission and acceptor excitation spectra.

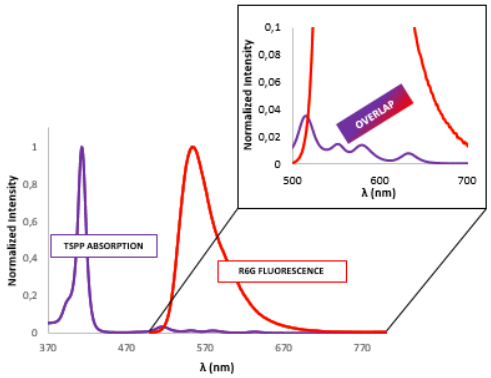

Figure 9. Normalized intensity spectra for TSPP absorption and R6G emission (λexc=483nm).

In order to obtain Spectral overlap integral, J ($M^{-1}cm^{-1}nm^4$)=6.67E+14 and calculate the critical distance, R0 (Å)=42.36-45.90 , the following parameters were used $\varepsilon_A(\lambda)$= 2.00E+4 $M^{-1}cm^{-1}$, κ^2= 2/3, n= 1.5-1.33, ϕ_D= 0.75. Therefore, the efficiency comes E(%)=30.95238-30.952381, and the distance between FRET couple porphyrin/rhodamine r(Å)=52,46824-48,4216729. Being proved that there's higher efficiency FRET in MCs, because of the shortening distances between TSPP and R6G molecules in the PE matrix of MCs.

Release of TSPP

The local concentration of TSPP is an important parameter to ensure the success of the efficiency of MCs as drug delivery systems.The hybrid CaCO3(PSS)(PAH)(PSS)(R6G)(PAH)(TSPP)(PSS) system, and CaCO3(PSS)(PAH)(PSS)(PAH)(TSPP) porphyrin system were studied. For the release performed at physiological pH=7.2, the MCs were suspended in a salt release solution NaH2PO4.H2O 0,68% (w/v), under stirring with media renovation. [6]

Table 1. Release results for the porphyrin and hybrid MCs, neutral pH, with media reposition.

System	$TSPP_{release}$ (nmol)	% Release	$S = \sqrt{\sigma^2}$
CaCO3(PSS)(PAH)3(PSS)(PAH)(TSPP)(PSS)	0.277	0.6	0,03 02
$CaCO3(PSS)(PAH)_3(PSS)(R6G)(PAH)(TSPP)(PSS)$	3.2	6.6	0,06 23

The release of TSPP in a neutral pH media is not an efficient one, as indicated by the values obtained and presented in table 8. The porphyrin of the hybrid system is coated between layers of different charged PE, PAH and PSS orderly. For the matrix of these capsules it might be steadier for the system the affinity of both opposite charged PEs to come closer in the matrix and to release some porphyrin into the media. Nevertheless, this quantity is very low (~6.6%) comparing with the adsorbed mass of porphyrin (0.0484μmol). Both confocal microscopy and FLIM images after release (b) and (d) display a disorganized/ruptured structure.

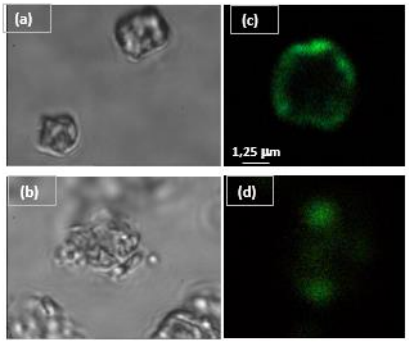

Figure 10. Confocal microscopy images (A and B) and FLIM images of hybrid MCs (C and D) obtained using laser excitation at λ_{exc}=483 nm.

General Conclusions and Future Remarks

The experimental work described in this Thesis is arranged in the temporal order of the sequential studies that have been done. The subjects range from the simple aqueous solution TSPP's and R6G's behaviour with PEs, to layer-by-layer polyelectrolyte, rhodamine, and porphyrin colloidal coated templates of $CaCO_3$. Three systems were designed, the porphyrin coated MCs, the rhodamine coated MCs and the hybrid, with both R6G and TSPP. For the use in PDT, the hybrid system maintain the monomer form of the porphyrin, adsorption onto the colloidal PSS and PAH matrix template prevented self-quenching, but the release of the porphyrin in neutral environments mimicking the intestinal region (followed at pH 7.2) shown high stability of the system with low release values. It is important to refer that other metabolic processes such as enzymatic activity, endocytosis or organism mechanical degrading mechanisms might as a hypothesis degrade the MCs, resulting in higher yielding release efficiencies when studying in vivo trials. The release of these MCs systems was not studied in acidic pHs, but some considerations can be done relying this future remark for the present experimental work. Low pH would eventually degrade de $CaCO_3$ core of the polyelectrolyte MCs, resulting in neutralization of the media pH and formation of CO_2, promoting the capsule collapse. The overall impact of this behaviour would be the promotion of the porphyrin release. The enhancement of the porphyrin's emission was observed. FLIM images revealed the existence of energy transference from the donor molecules of R6G entrapped in the PE matrix of the MCs and the acceptor molecules of TSPP, by FRET mechanism. Comparing with the same system in aqueous solution, in which there is no excitation energy transfer, the hybrid system pointed to the importance of the distance reduction between donor and acceptor molecules, and the strategic role of the polyelectrolyte matrix, orientating the transition dipole's of the rhodamine and the porphyrin in such a way that the FRET mechanism is efficient. When in vivo, the rhodamine, upon irradiation, would transfer its energy to the acceptor molecule of the porphyrin, which then follows a Type II photochemical process involving an energy transfer between excited triplet state of the PS and stable triplet oxygen, resulting in ROS that can evoke some cell death pathways. During the layer-by-layer assembly of the MCs, it was detected substantial loss of rhodamine in the washing steps, the electrostatic interaction with the PE matrix wasn't strong enough to prevent some detachment of this small sized dye with high diffusion constant. In the future, the design of MCs with different templates, PEs,

as well as different dye/porphyrin couples might be interesting.

ACKNOWLEDGEMENTS

My academic path was marked by extraordinary people for whom I'd like to express my sincere gratitude. My supervisor Dr. Suzana Paiva showed patience and kind advices which were crucial for transference of knowledge. I would also like to thank Dr. Vanda Serra and Dr. Pedro Paulo for their availability. I also would like to acknowledge project PTDC/QUI-COL/29379/2017. To all the teachers, and classmates essential through this journey.

BIBLIOGRAPHY

[1] World Health Organization. (2018).Global cancer data. International. Agency for Research on. cancer, 13–15.

[2] Tsolekile, N., Nelana, S., & Oluwafemi, O. S. (2019). Porphyrin as Diagnostic and Therapeutic Agent. *Molecules (Basel, Switzerland)*, *24*(14), 2669.

[3] del Mercato, L. L., Ferraro, M. M., Baldassarre, F., Mancarella, S., Greco, V., Rinaldi, R., & Leporatti, S. (2014). Biological applications of LbL multilayer capsules: from drug delivery to sensing. *Advances in colloid and interface science*, *207*, 139–154.

[4] Valeur, B. (2001). Molecular Fluorescence: Principles and Applications. Wiley-VCH Verlag GmbH & Co. KGaA.

[5] Serra, S., Inteligent polymeric microcapsules of nano hybrids of porphyrin-gold to apply on Photodynamic Therapy and Bioimaging, 2019, IST.

[6] Neto, N., Construction of Polyelectrolyte Microcapsules envisaging potential Cancer Therapy, 2017, IST.

[7] Teixeira, R., Serra, V.V., Paulo, P., Andrade, S., & Costa, S. (2015). Encapsulation of photoactive porphyrinoids in polyelectrolyte hollow microcapsules viewed by fluorescence lifetime imaging microscopy (FLIM). *RSC Advances, 5*, 79050-79060.

[8] S.M. Andrade, R. Teixeira, Sílvia M.B. Costa, A.J.F.N. Sobral. Self-aggregation of free base porphyrins in aqueous solution and in DMPC vesicles. Biophysical Chemistry, Elsevier, 2008, 133 (1-3)

[9] R. F. Kubin and A. N. Fletcher, J. Lumin. 27, 455 (1982). [53] Wang, C., He, C., Tong, Z., Liu, X., Ren, B., Zeng, F. (2006). Combination of adsorption by porous CaCO3 microparticles and encapsulation by polyelectrolyte multilayer films for sustained drug delivery. International Journal of Pharmaceutics, 308(1–2), 160–167.

[10] Sabri, I. N., Alias, N., Ali, A. M., Mohammed, J. S. (2016). Characterization of CaCO3 microspheres fabricated using distilled water. The Malaysian Journal of Analytical Sciences, 20(2), 423–435.

[11] Maleki Dizaj, S., Barzegar-Jalali, M., Zarrintan, M. H., Adibkia, K., Lotfipour, F. (2015) Calcium carbonate nanoparticles as cancer drug delivery system. Expert Opinion Drug Delivery, 12(10), 75 1649–1660.

[12] Bhattacharjee, S. (2016). DLS and zeta potential - What they are and what they are not. Journal of Controlled Release, 235, 337–35.